

Effect of iron impurities on the catalytic activity of BEA, MOR and MFI zeolites in the SCR of NO by ethanol

Stanislaw Dzwigaj^{a,b,*}, Janusz Janas^c, Wojciech Rojek^c, Lorenzo Stievano^{a,b}, Friedrich E. Wagner^d, Frédéric Averseng^{a,b}, Michel Che^{a,b,e}

^aUPMC Univ Paris 6, UMR 7609, Laboratoire de Réactivité de Surface, 4 Place Jussieu, 75252 Paris Cedex 05, France

^bCNRS, UMR 7609, Laboratoire de Réactivité de Surface, 4 Place Jussieu, 75252 Paris Cedex 05, France

^cInstitute of Catalysis and Surface Chemistry, Polish Academy of Sciences, ul. Niezapominajek 8, 30-239 Kraków, Poland

^dPhysik-Department E15, Technische Universität München, James-Frank-Strasse, 85747 Garching, Germany

^eInstitut Universitaire de France

ARTICLE INFO

Article history:

Received 30 April 2008

Received in revised form 10 July 2008

Accepted 19 July 2008

Available online 26 July 2008

Keywords:

BEA

MOR

MFI

Iron impurities

SCR of NO

XRD

EPR

Mössbauer

ABSTRACT

The combined use of chemical analysis, XRD, EPR and Mössbauer techniques provides detailed information on the nature of iron impurities in commercial BEA, MOR and MFI zeolites. EPR and Mössbauer spectroscopies evidence that iron impurities are present mainly as tetrahedral Fe(III) species and to a minor extent as octahedral Fe(III) species, with relative amounts depending on the type of zeolite. Iron impurities present in commercial BEA, MOR and MFI zeolites are active in the selective catalytic reduction (SCR) of NO by ethanol, with NO conversion higher than 37, 43 and 50% for BEA, MOR and MFI, respectively, and with selectivity toward N₂ higher than 90% for all zeolites in the temperature range 575–775 K. The much higher activity of commercial BEA, MOR and MFI than that of FeSiBEA and CoSiBEA, both prepared by a two-step postsynthesis method, suggests that Fe(III) impurities in commercial zeolites are present in tetrahedral and/or octahedral environments, possibly close to lattice Al, which make them active in the SCR of NO by ethanol. The Brønsted and Lewis acidic sites in studied zeolites are determined by FTIR measurements of pyridine adsorption.

© 2008 Elsevier B.V. All rights reserved.

1. Introduction

Transition metal-based zeolites are active in many catalytic reactions including oxidative dehydrogenation of alkanes [1–3], selective oxidation of benzene to phenol [4], selective catalytic reduction (SCR) of NO by hydrocarbons or ammonia [5–24] and direct N₂O decomposition [25,26]. Their catalytic performances depend on several parameters, particularly the chemical state of transition metal impurities present in the zeolite structure [27,28].

Recently, in the framework of potential applications of transition metal-based catalysts for the effective control of NO_x emission, considerable effort has been devoted to the understanding of SCR of NO by various reducing agents [29–40]. However, despite numerous

papers on transition metal-based zeolites [5–24,41], the nature of the active sites is still a matter of discussion. Several types of metal sites have been discussed in transition metal-based zeolites such as isolated lattice and extra lattice metal species, metal oligomers and metal oxides. Moreover, lattice and extra lattice Al species as well as transition metal impurities such as iron can be also involved as active sites.

To the best of our knowledge the role of iron impurities, commonly found in zeolites such as BEA, MOR and MFI, on their catalytic activity in the SCR of NO by ethanol has not been reported yet.

For sake of comparison, partly and completely dealuminated BEA zeolites, containing small amounts or no iron impurities as well as MOR and MFI zeolites were also investigated. This work is also relevant to other catalytic reactions, such as oxidative dehydrogenation of alkanes or selective oxidation of different organic molecules.

In this work, the Brønsted and Lewis acidic sites in studied zeolites are determined by IR measurements of pyridine adsorption.

* Corresponding author at: UPMC Univ Paris 6, CNRS UMR 7609, Laboratoire de Réactivité de Surface, 4 Place Jussieu, 75252 Paris Cedex 05, France.

Tel.: +33 1 44 27 52 91; fax: +33 1 44 27 60 33.

E-mail address: stanislaw.dzwigaj@upmc.fr (S. Dzwigaj).

Table 1
Preparation parameters, Si/Al ratio, Fe content and textural properties of zeolite samples

Sample	Treatment HNO ₃ (conc./time)	Si/Al	Fe content (ppm)	Micropore volume (cm ³ g ⁻¹)	Surface area (m ² g ⁻¹)
HAIBEA(7 0 0) ^a	Not treated	11	700	0.25	660
HAIBEA(3 0 0) ^b	Not treated	12.5	300	0.25	640
HAISiBEA(1 0 0) ^c	6 M/4 h	377	100	0.24	650
SiBEA ^c	13 M/4 h	1000	Not detected	0.24	655
MOR(1 5 0)	Not treated	5	150	0.20	470
MFI(3 0 0)	Not treated	25	300	0.15	340

^a The parent TEABEA zeolite (Si/Al = 11) was calcined in flowing air at 823 K for 15 h to remove the tetraethylammonium (TEA) template.

^b The parent TEABEA zeolite (Si/Al = 12.5) was calcined in flowing air at 823 K for 15 h to remove the tetraethylammonium (TEA) template.

^c The initial sample was HAIBEA(7 0 0).

2. Experimental

2.1. Samples preparation

Two tetraethylammonium BEA (TEABEA) zeolites with Si/Al = 11 and 12.5 provided by RIPP (China) were found to contain 700 and 300 ppm of Fe impurities respectively (Table 1). They were calcined at 823 K for 15 h in flowing air to obtain organic-free samples and labeled HAIBEA(7 0 0) and HAIBEA(3 0 0) respectively. HAIBEA(7 0 0) with surface area of 660 m² g⁻¹ and micropore volume of 0.25 cm³ g⁻¹ was separated into two fractions. The first was treated with 6 mol L⁻¹ to obtain HAISiBEA(1 0 0) with Si/Al = 377, surface area of 650 m² g⁻¹ and micropore volume of 0.24 cm³ g⁻¹. It contained 100 ppm of Fe. The second was treated with 13 mol L⁻¹ HNO₃ for 4 h at 353 K to obtain practically Fe-free SiBEA with Si/Al = 1000, surface area of 655 m² g⁻¹ and micropore volume of 0.24 cm³ g⁻¹.

For the sake of comparison, commercial mordenite with surface area of 470 m² g⁻¹, micropore volume of 0.20 cm³ g⁻¹ and Si/Al = 5 and ZSM-5 zeolite with surface area of 340 m² g⁻¹, micropore volume of 0.15 cm³ g⁻¹ and Si/Al = 25 were also used in this work. These zeolites contained 150 and 300 ppm Fe impurities were labeled MOR(1 5 0) and MFI(3 0 0), respectively (Table 1).

2.2. Characterisation

The iron content was obtained by chemical analysis (Service Central d'Analyse de CNRS, Vernaison, France).

X-ray powder diffractograms were recorded on a Siemens D5000 diffractometer using Cu K α radiation (λ = 154.05 pm).

EPR spectra were recorded at 298 and 77 K on a Bruker ESP 300 spectrometer at 9.3 GHz (X-band) with a 100-kHz field modulation and a modulation amplitude of 10 Gauss.

⁵⁷Fe Mössbauer spectra were measured at 4.2 K with a ⁵⁷Co/Rh source in a liquid helium bath cryostat. The spectrometer is operated with a sinusoidal velocity waveform. The spectra were fitted with appropriate sets of Voigt profiles using the MOS-90 computer program [41,42]. Mössbauer parameters such as magnetic hyperfine field B_{hf} , electric quadrupole splitting QS and isomer shift IS relative to α -Fe metal [41,42] are gathered in Table 2.

Transmission FT-IR spectra of samples as self-supported wafers (20 mg) were recorded at 298 K on a Bruker IFS 66 V spectrometer, with a resolution of 2 cm⁻¹. Before measurements, the wafers were dehydrated in flowing oxygen (120 ml min⁻¹, 8 h) to 773 K (heating rate of 100 K h⁻¹) then evacuated for 6 h at 573 K in the IR cell. Gaseous pyridine was introduced on dehydrated wafers and the physisorbed part eliminated by evacuation at 423 K for 1 h.

2.3. Catalysis measurements

The catalytic activity in the SCR of NO by ethanol was measured in a conventional plug flow reactor coupled to a gas chromatograph

Table 2
⁵⁷Fe Mössbauer parameters at 4.2 K of different zeolite samples

Sample ^a	B_{hf} ^b (T)	QS ^c (mm s ⁻¹)	IS ^d (mm s ⁻¹)	Area (%)	Site ^e
HAIBEA(7 0 0)	53.3(3)	-0.03(5)	0.29(3)	100	Fe(III)-SPR
HAIBEA(3 0 0)	53.7(2)	-0.06(4)	0.29(2)	100	Fe(III)-SPR
MOR(1 5 0)	54.5(5)	-0.02(6)	0.26(6)	100	Fe(III)-SPR
MFI(3 0 0)	54.4(4)	-0.03(6)	0.27(5)	100	Fe(III)-SPR

^a Sample description as in text.

^b Magnetic hyperfine field.

^c Electric quadrupole splitting.

^d Isomer shift values given by reference to α -Fe metal.

^e Fe(III)-SPR: iron undergoing slow paramagnetic relaxation.

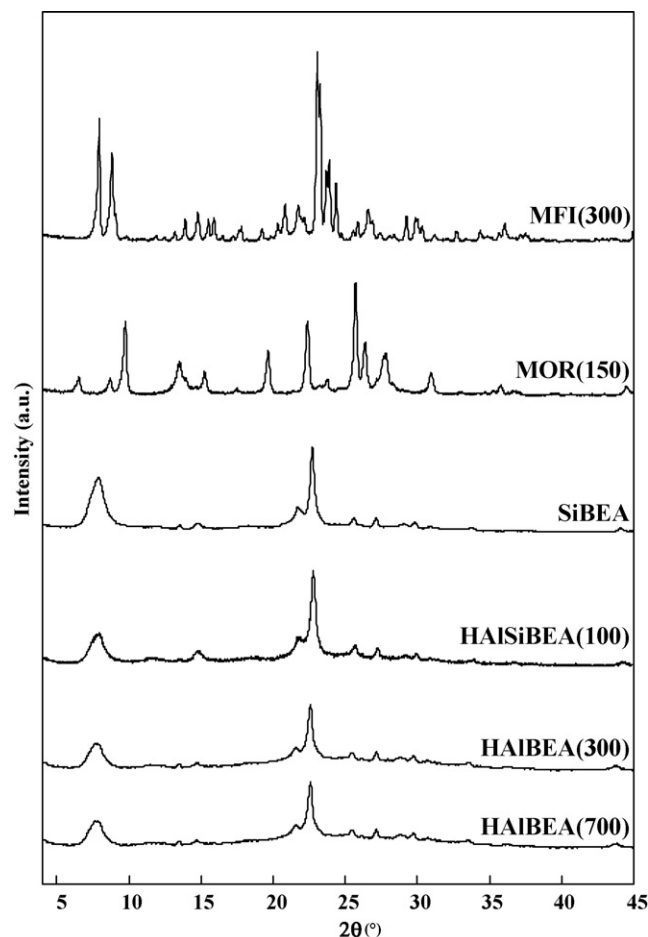


Fig. 1. X-ray diffractograms recorded at room temperature and ambient atmosphere of HAIBEA(7 0 0), HAIBEA(3 0 0), HAISiBEA(1 0 0), SiBEA, MOR(1 5 0) and MFI(3 0 0).

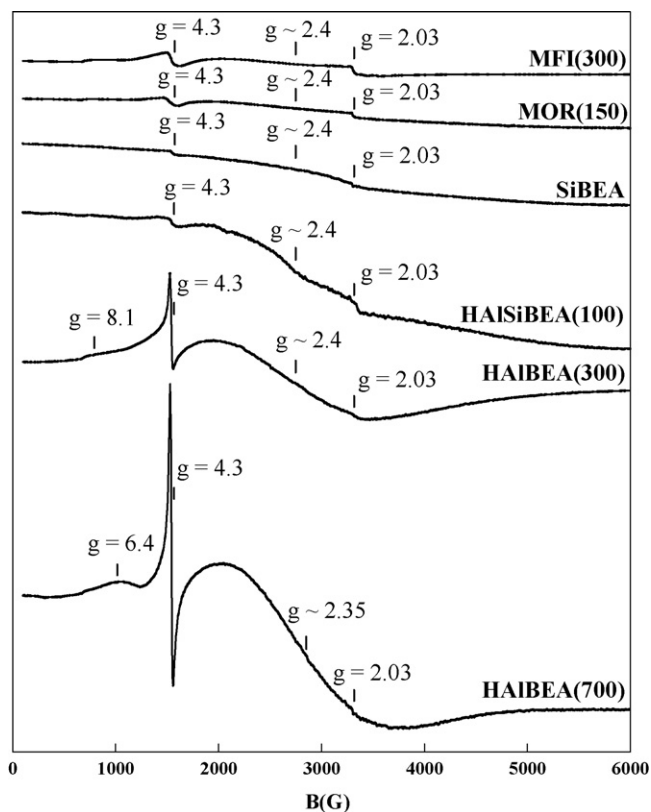


Fig. 2. EPR spectra (X-band) recorded at 77 K and ambient atmosphere of HAlBEA(7 0 0), HAlBEA(3 0 0), HAlSiBEA(1 0 0), SiBEA, MOR(1 5 0) and MFI(3 0 0).

and a continuous NO_x detector. The composition of the feed was: 1000 ppm NO, 1000 ppm ethanol and 2 vol.% O_2 with a catalyst volume of 0.5 ml and a gas hour space velocity (GHSV) of $10,000 \text{ h}^{-1}$. In a standard experiment, the catalyst samples were pretreated at 523 K in an oxygen/helium mixture before switching on the NO and ethanol vapour streams. The standard catalytic conditions consisted of a step of 2 h at 523 K, then the temperature was increased every 50 K intervals up to 773 K (temperature ramp 100 K h^{-1}). The temperature was then lowered regularly in the same manner. The NO_x and CO_x concentrations were monitored at the reactor outlet for checking if pseudo steady-state conditions were established. NO conversion hysteresis were practically absent during the catalytic tests.

The conversion and selectivity values, defined and calculated in a standard manner, are given in mol%. Because of the difficulty to determine the N_2 concentration at the reactor outlet, the selectivity toward N_2 was determined as follows:

$$S_{\text{N}_2}[\%] = 100 - (S_{\text{NO}_2} + S_{\text{N}_2\text{O}} + S_{\text{NH}_3} + S_{\text{OrgN}})$$

where S_{NO_2} , $S_{\text{N}_2\text{O}}$ and S_{NH_3} is the selectivity toward NO_2 , N_2O and ammonia, respectively, and S_{OrgN} is sum of the selectivities toward nitrogen-containing organic compounds.

3. Results and discussion

3.1. Nature and environment of iron impurities in zeolites

3.1.1. X-ray diffraction

As shown earlier [43,44], the treatment with nitric acid does not alter the crystallinity of BEA zeolite, leading to similar XRD patterns for HAlBEA(7 0 0), HAlBEA(3 0 0), HAlSiBEA(1 0 0) and SiBEA samples (Fig. 1). The narrow diffraction peak located near

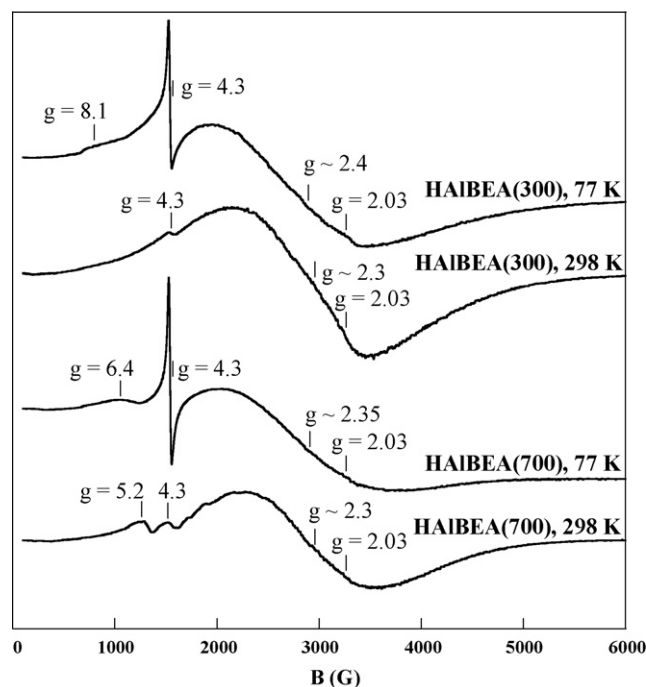


Fig. 3. EPR spectra (X-band) recorded at 77 and 298 K and ambient atmosphere of HAlBEA(7 0 0) and HAlBEA(3 0 0).

22.6° , which intensity significantly increases upon dealumination, corresponds to d_{302} reflection and can be employed to follow the contraction of the BEA matrix [45,46]: thus the average d_{302} spacing decreases upon dealumination from 3.942 Å (HAlBEA(7 0 0) and HAlBEA(3 0 0) samples) ($2\theta = 22.55^\circ$) to 3.912 Å ($2\theta = 22.71^\circ$) (SiBEA sample).

X-ray diffractograms of MOR(1 5 0) and MFI(3 0 0) are characteristic for XRD pattern of mordenite and ZSM-5 zeolite, respectively.

3.1.2. Electron paramagnetic resonance spectroscopy

Fig. 2 shows the EPR spectra recorded at 77 K of the various zeolite samples. The EPR spectra of HAlBEA(7 0 0) and HAlBEA(3 0 0) which are very similar show four signals at $g = 6.4$ (8.1 for HAlBEA(3 0 0)), 4.3, 2.4–2.35 and 2.03. The assignment of such signals frequently detected in Fe-containing zeolites [47–52] is not straightforward. The number and position of EPR signals for Fe(III) species observable in a powder spectrum mainly depend on the local symmetry of these species and their possible magnetic interactions.

As proposed earlier for Fe-containing zeolites [50–55], the signal at $g = 4.3$ may be assigned to tetrahedral Fe(III) ions at lattice sites, that at $g = 8.1/6.4$ to isolated Fe(III) ions in penta- and/or octahedral coordination, the broad signal at $g \sim 2.4$ –2.35 to iron oxide clusters and the signal at $g = 2.03$ to Fe(III) ions in octahedral environment either isolated or within FeO_x oligomers.

Similar signals are observed at 298 K (Fig. 3). The signals at $g \sim 2.4$ –2.35 with narrower line width and higher intensity and these at $g = 2.03$ with lower intensity than those recorded at 77 K appear. Since for isolated, highly symmetric Fe(III) species, the signal intensity follows the Curie–Weiss law, i.e. $I \sim 1/T$ [47], this points to antiferromagnetic interactions that disappear upon heating and suggests that the broad line observed particularly for HAlBEA(7 0 0) and HAlBEA(3 0 0) at $g \sim 2.4$ arises from neighbouring Fe(III) species rather than from isolated ones [47].

For MOR(1 5 0) and MFI(3 0 0), similar EPR signals at $g = 8.1$, 4.3, 2.4 and 2.03 are observed at 77 and 298 K, with however much lower

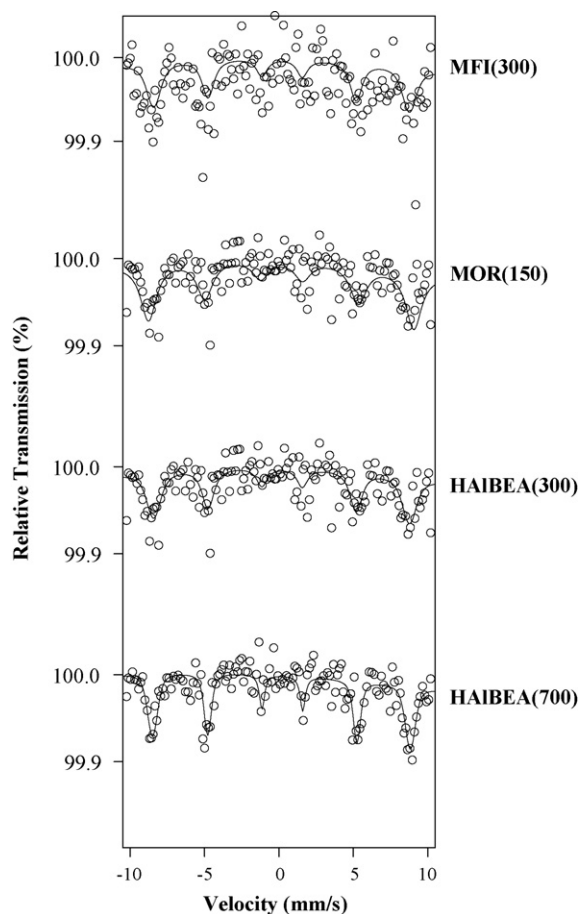


Fig. 4. ^{57}Fe Mössbauer spectrum recorded at 4.2 K and ambient atmosphere of HAIBEA(3 0 0), HAIBEA(7 0 0), MOR(150) and MFI(3 0 0).

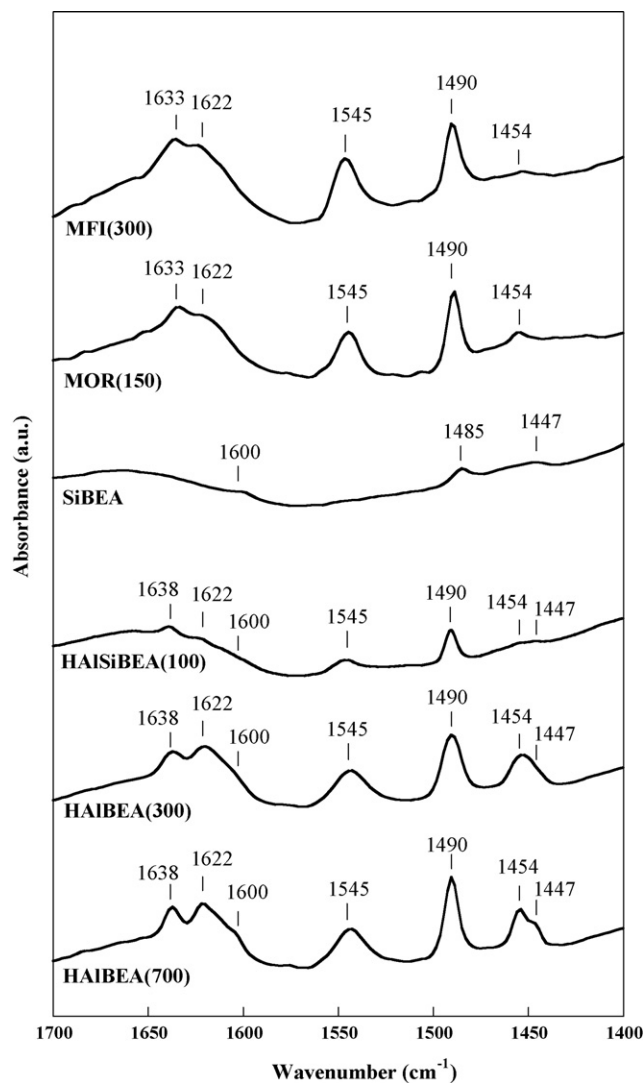


Fig. 5. FTIR spectra recorded at room temperature of HAIBEA(7 0 0), HAIBEA(3 0 0), HAISiBEA(1 0 0), SiBEA, MOR(1 5 0) and MFI(3 0 0) calcined at 773 K for 8 h in flowing air and then outgassed at 573 K for 6 h (10^{-3} Pa) in the IR cell.

intensity than for HAIBEA(7 0 0) and HAIBEA(3 0 0). The signal at $g = 2.03$ is very weak in all studied samples, indicating that iron oxide clusters are practically absent in commercial zeolites and that Fe(III) ions are mostly present at isolated tetrahedral lattice sites. However, it seems that very small amount of iron oxide clusters appear which could be evidenced by the broad signal at $g = \sim 2.4$ (Fig. 2), in line with earlier report [47]. However, the ^{57}Fe Mössbauer spectra do not indicate the presence of such type of Fe species, as shown in the next section.

The very small iron loading of HAISiBEA(1 0 0) is consistent with its EPR spectrum in the same way as dealuminated SiBEA sample (Si/Al = 1000) with practically no iron impurities (Fig. 2).

3.1.3. ^{57}Fe Mössbauer spectroscopy

Fig. 4 shows the ^{57}Fe Mössbauer spectra at 4.2 K of HAIBEA(7 0 0), HAIBEA(3 0 0), MOR(1 5 0) and MFI(3 0 0).

The poor signal-to-noise ratio observed is due to the very low iron loading. Consequently, the use of more than one single spectral component representing the average of different possible iron sites does not significantly improve the fit (its quality has been checked by the χ^2 parameter [41,42]). The spectral parameters obtained with this procedure are gathered in Table 2.

In all spectra, the only visible component is a magnetic sextet. Because of the very low iron content and considering the very high value of the magnetic field of the hyperfine sextet and the quasi absence of quadrupole splitting, it is possible to assign the sextets

to isolated Fe(III) species undergoing slow paramagnetic relaxation [56,57]. This effect is often observed for highly dilute Fe(III) ions, with no exchange-coupled pairs.

In addition, the value of IS for this component lies between those typically observed for tetrahedral and octahedral Fe(III) ions, even though it is closer to the tetrahedral ones. This result suggests that such isolated Fe(III) ions mainly occupy tetrahedral sites in the zeolite framework, the slight variation in isomer shift reflecting different distributions of the iron sites in the samples.

In the case of Al-containing H-BEA zeolite, opening of framework linkages can occur upon hydration, leading to reversible formation of octahedral framework Al species with simultaneous loss of framework Brønsted (and therefore of cationic exchange) sites [58]. Therefore, the presence of octahedrally coordinated iron does not necessarily imply the existence of extra lattice iron species. On the contrary, the high dilution of Fe(III) ions rather suggests the presence of octahedral lattice Fe(III) ions that form upon hydration, which are reversibly back transformed into tetrahedral Fe(III) species upon dehydration.

These observations agree with our earlier work on Fe-containing SiBEA zeolite prepared by two-step postsynthesis method, with Fe incorporated in tetrahedral and octahedral lattice sites [59].

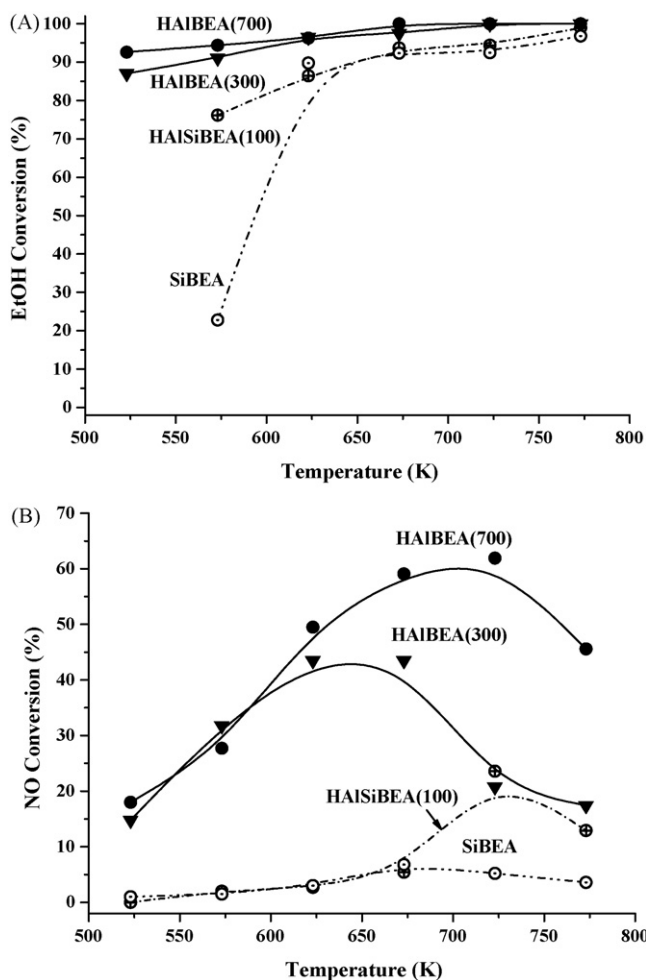


Fig. 6. Temperature-dependence of (A) ethanol and (B) NO conversion in SCR of NO by ethanol on BEA samples with different Fe impurity content: HAIBEA(700) (full circles), HAIBEA(300) (triangles), HAlSiBEA(100) (crossed circles), SiBEA (empty circles).

3.1.4. FTIR spectroscopy and pyridine adsorption

To check the acidity of studied materials, pyridine is adsorbed at room temperature on the samples calcined at 773 K for 8 h in flowing air and then outgassed at 573 K for 6 h (10^{-3} Pa) in the IR cell. FTIR spectra are recorded after desorption of pyridine at 423 K for 1 h. The IR bands typical of pyridinium cation are observed at 1545 and $1633\text{--}1638\text{ cm}^{-1}$ for dehydrated HAIBEA(700), HAIBEA(300), HAIBEA(100), MOR(150) and MFI(300), indicating presence of Brønsted acidic sites (Fig. 5). Moreover, for these samples the band at 1454 cm^{-1} appears characteristic of pyridine bonded to strong Lewis acidic sites.

In contrast, these bands are not observed for SiBEA indicating absence of Brønsted and strong Lewis acidic sites. Only the bands at 1600, 1485 and 1447 cm^{-1} appear (Fig. 5) related to pyridine interacting with weak Lewis acidic sites and/or pyridine physisorbed, in line with earlier reports [60–62].

3.2. Effect of Fe impurities on the catalytic properties of BEA, MOR and MFI zeolites

The SCR activity of commercial BEA, MOR and MFI zeolites (Figs. 6–10) is high in the 523–773 K range. The maximum NO_{SCR} conversion (where NO_{SCR} denotes NO conversion in SCR process) of HAIBEA(700) is of 59–62% in the 673–723 K range, with a

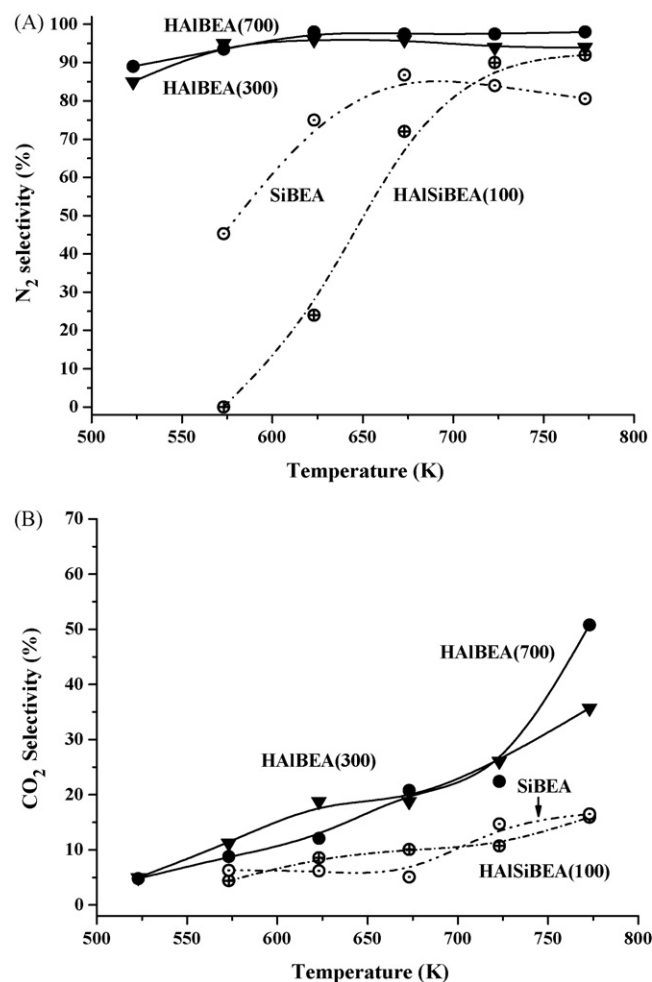


Fig. 7. Temperature-dependence of (A) N₂ and (B) CO₂ selectivity in SCR of NO by ethanol on BEA samples with different Fe impurity content: symbol denotation as in Fig. 6.

selectivity toward N₂ exceeding 90%. HAIBEA(300) with less Fe is slightly less active, with 44% NO conversion in the 623–673 K range. NO_{SCR} conversion for commercial MOR and MFI zeolites is close to that for HAIBEA(300) what could be related to the Fe impurity level in those zeolites. The ethanol conversion is very high and even at 523 K exceeds 85%. Taking into consideration of the ethanol excess in the feed in respect to NO reduction demand it is obvious that part of ethanol is oxidized by gaseous oxygen and this process is competitive to SCR of NO.

In the same time the selectivity toward N₂ is quite high for the all commercial samples (Figs. 6–10) but ethanol oxidation evidently proceeds through the intermediate steps that is reflected by the temperature dependence of CO₂ selectivity. As the detailed reaction mechanism is not found, the temperature dependence lines of conversion and product selectivities for the investigated samples are not fitted but rather show trends in all presented figures.

The catalysis results obtained for HAIBEA(700) (Fig. 8), indicate that, at all reaction temperatures, NO conversion is higher with than without ethanol. This observation agrees with earlier work on Fe_xSiBEA or Co_xSiBEA [15,24]: mononuclear tetrahedral Fe and Co ions are responsible for their high activity in the SCR of NO by ethanol leading to N₂ and the oxidation of NO to NO₂ is not a necessary intermediate step. This conclusion is supported by several papers and not exclude that adsorbed NO_x species may be

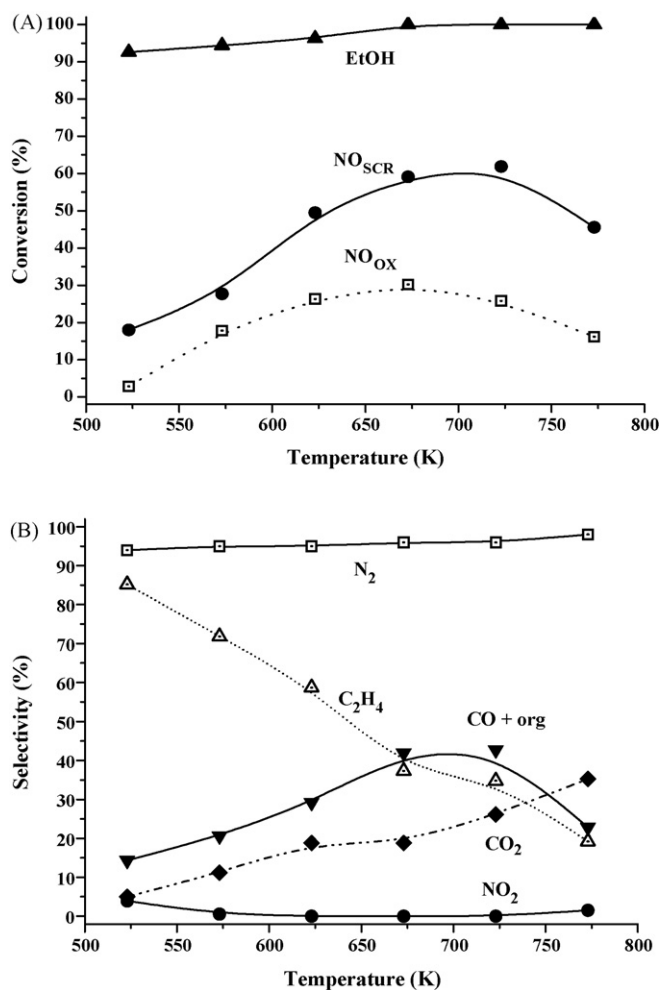


Fig. 8. Temperature-dependence of (A) ethanol (triangles) and NO conversions (NO_{SCR} (full circles), NO_{OX} (empty squares)) and (B) product selectivities (dinitrogen (empty squares), ethylene (empty triangles), CO and organic intermediates (full triangles), CO₂ (full rombs) and NO₂ (full circles) in SCR of NO by ethanol in HAlBEA(7 0 0).

intermediate products of NO SCR process [63–66]. The selectivity toward NO₂ is very low in the whole temperature range and low amounts of N₂O (not given on the Fig. 8) complete the nitrogen compounds balance at 573 K for HAlBEA(7 0 0) and HAlBEA(3 0 0).

For all investigated samples, ethanol conversion considerably higher than that of NO never reaches 100%. In addition to ethanol, some other organic products, such as ethylene, CO, aldehydes and traces of acetonitrile are formed for all samples at 523 K. This

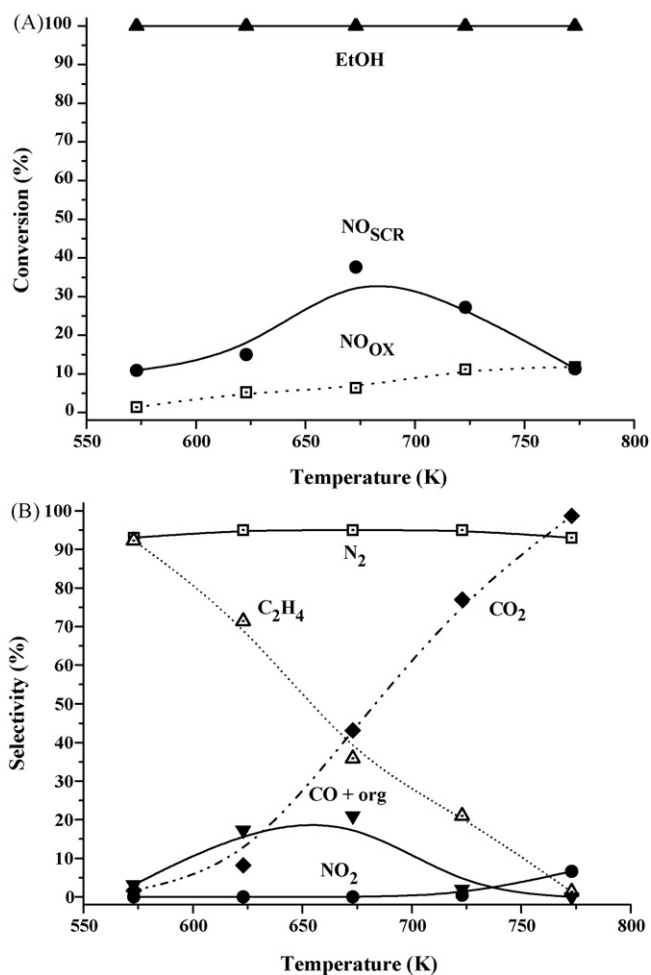


Fig. 9. Temperature-dependence of (A) ethanol and NO conversions and (B) product selectivities in SCR of NO by ethanol on MOR(150): symbol denotation as in Fig. 8.

observation is similar to that previously made for Fe_xSiBEA and Co_xSiBEA catalysts, where the presence of active organic compounds was suggested to be necessary to obtain both high NO conversion and high selectivity toward N₂.

In low reaction temperature range the main product is ethylene, probably formed on the acidic centres evidenced in all commercial zeolites by pyridine adsorption (Fig. 5). The ethylene, CO and organic intermediates (acetaldehyde, diethyl ether and acetonitrile found in minor amount) could themselves serve as reducing agents in SCR of NO process after depletion of ethanol molecules in the reaction zone. These compounds hinder

Table 3

NO conversion and selectivity toward N₂ in SCR of NO by ethanol on BEA zeolites with different Fe impurity content (HAlBEA(7 0 0) and HAlBEA(3 0 0)) and Fe_{0.3}SiBEA and Fe_{0.9}SiBEA obtained by two-step postsynthesis method [15,46]

T _R (K) ^a	C _{NO} (%) ^b				S _{N₂} (%) ^c			
	HAlBEA(7 0 0)	HAlBEA(3 0 0)	Fe _{0.3} SiBEA	Fe _{0.9} SiBEA	HAlBEA(7 0 0)	HAlBEA(3 0 0)	Fe _{0.3} SiBEA	Fe _{0.9} SiBEA
523	18.0	14.8	6.2	22.2	89.1	84.8	62.2	79.7
573	27.7	31.8	16.8	55.8	93.5	94.8	85.3	93.9
623	49.5	43.5	21.8	48.2	97.8	96.1	92.3	96.8
673	59.1	43.5	28.2	39.1	97.5	95.7	94.1	96.0
723	61.9	20.8	14.0	30.1	97.6	94.2	84.3	95.7
773	45.6	17.4	10.2	22.2	97.8	93.8	66.3	91.8

HAlBEA samples description as in text. Fe_{0.3}SiBEA, Fe_{0.9}SiBEA are FeSiBEA samples with 0.3 and 0.9 wt.% of Fe, respectively.

^a Reaction temperature of SCR of NO by ethanol.

^b NO conversion.

^c Selectivity toward N₂.

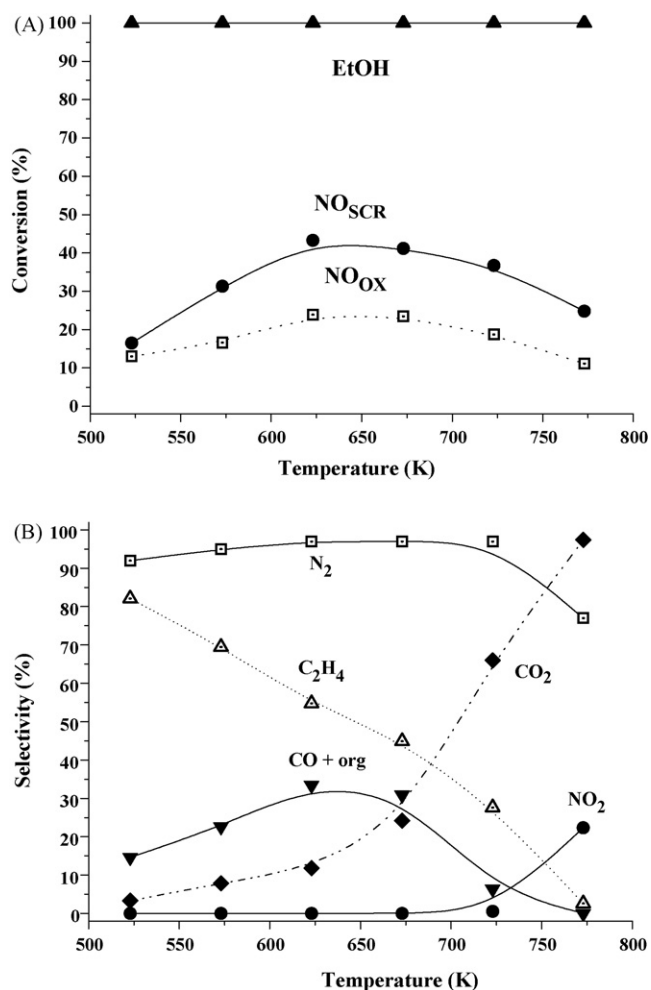


Fig. 10. Temperature-dependence of (A) ethanol and NO conversions and (B) product selectivities in SCR of NO by ethanol on MFI(3 0 0): symbol denotation as in Fig. 8.

in the same time the gaseous NO₂ formation, even in the high reaction temperature range.

The NO conversion on BEA samples (Fig. 6B) decreases with the Fe(III) ions content, removed upon dealumination of HAlBEA. At the same time, the overall oxidation activity slightly decreases. This result is likely to be connected to the content of Fe still present in the zeolite structure. The residual weak activity in the SCR of NO for HAlSiBEA(1 0 0) above 673 K (Fig. 6B) indicates that some less active reaction sites remain present in the zeolite even after removal of most Fe(III) ions. The remaining Al lattice ions (and the corresponding protons at exchangeable positions) may be responsible for this high temperature activity.

After almost total removal of Fe impurities and complete dealumination, sample SiBEA is practically inactive in the SCR of NO with ethanol being mostly converted to ethylene. It seems, that the higher N₂ selectivity of SiBEA than HAlSiBEA is probably related to the presence in the former sample only traces of isolated tetrahedral Fe(III) species active in SCR of NO toward N₂ and the presence in the latter one not only isolated tetrahedral Fe(III) species but also isolated octahedral Fe(III) and/or very small amount of iron oxide clusters active in NO oxidation to NO₂, in line with our earlier work on Fe_xSiBEA zeolites [15].

The comparison of activities of HAlBEA(7 0 0) and HAlBEA(3 0 0) with Fe_xSiBEA obtained by a two-step postsynthesis method [15] with much higher Fe content (0.9 Fe wt.%), shows that

the former zeolites are more active than the latter, and that their selectivity toward N₂ reaches higher values in a wider temperature range (Table 3). These results suggest that Fe(III) impurities are present in commercial zeolites in a tetrahedral and/or octahedral environments, possibly close to lattice Al, which make them more active than Fe(III) species present in siliceous Fe_xSiBEA zeolite.

4. Conclusion

The combined use of chemical analysis, XRD, EPR and Mössbauer provides detailed information on the nature of iron impurities in commercial BEA, MOR and MFI zeolites. Iron impurities are mainly present as tetrahedral Fe(III) species but also as octahedral Fe(III) which relative amounts depend on the type of zeolite, as shown by EPR and Mössbauer.

The iron species present in BEA are active in the SCR of NO by ethanol at 575–775 K, with NO conversion higher than 50% and a selectivity toward N₂ higher than 90%.

The high activity of iron impurities at 575–775 K is not limited to BEA zeolite but also to mordenite (MOR(1 5 0)) and MFI(MFI(3 0 0)) zeolites. Both MOR(1 5 0) and MFI(3 0 0) show NO conversion of 37.5 and 43%, respectively, and 90–100% selectivity toward N₂.

The much higher activity for commercial BEA, MOR and MFI zeolites compared to Fe_xSiBEA [15] obtained by two-step post-synthesis method, suggests that Fe(III) impurities present in commercial zeolites in a tetrahedral and/or octahedral environments, are possibly close to lattice Al, which make them more catalytically active than Fe(III) ions in siliceous Fe_xSiBEA zeolite.

Further studies are foreseen to better understand the role of lattice Al ions on the catalytic activity in SCR of NO by ethanol and propane.

References

- [1] P.B. Venuto, *Microporous Mater.* 2 (1994) 297.
- [2] M.D. Uddin, T. Komatsu, T. Kashima, *J. Catal.* 150 (1994) 439.
- [3] K.A. Dubkov, V.I. Sibolev, G.I. Panov, *Kinet. Catal.* 39 (1998) 72.
- [4] G.I. Panov, A.K. Uriarte, M.A. Rodkin, V.I. Sobolev, *Catal. Today* 41 (1998) 365.
- [5] X. Feng, W.K. Hall, *Catal. Lett.* 41 (1996) 45.
- [6] M. Iwamoto, T. Zengyo, A.M. Hernandez, H. Araki, *Appl. Catal. B* 17 (1998) 259.
- [7] H.Y. Chen, W.M.H. Sachtler, *Catal. Today* 42 (1998) 73.
- [8] G. Centi, F. Vazanna, *Catal. Today* 53 (1999) 683.
- [9] A.Z. Ma, W. Grünert, *J. Chem. Soc., Chem. Commun.* (1999) 71.
- [10] R. Burch, S. Scire, *Appl. Catal. B* 3 (1994) 295.
- [11] T. Beutel, Z. Zhang, W.M.H. Sachtler, H. Knözinger, *J. Phys. Chem.* 97 (1993) 3579.
- [12] Y. Li, J.N. Armor, *Appl. Catal. B* 2 (1993) 239.
- [13] M. Haneda, Y. Kintaichi, H. Shimada, H. Hamada, *J. Catal.* 192 (2000) 137.
- [14] M. Haneda, Y. Kintaichi, H. Mizushima, N. Kakuta, H. Hamada, *Appl. Catal. B* 31 (2001) 81.
- [15] S. Dzwigaj, J. Janas, T. Machej, M. Che, *Catal. Today* 119 (2007) 133.
- [16] T. Tabata, M. Kokitsu, H. Ohtsuka, O. Okada, L.M.F. Sabatino, G. Bellussi, *Catal. Today* 27 (1996) 91.
- [17] H. Ohtsuka, T. Tabata, O. Okada, *Catal. Today* 42 (1998) 45.
- [18] T. Tabata, H. Ohtsuka, L.M.F. Sabatino, G. Bellussi, *Microporous Mesoporous Mater.* 21 (1998) 517.
- [19] S.C. Shen, S. Kawi, *J. Catal.* 213 (2003) 241.
- [20] H.H. Chen, S.C. Shen, X. Chen, S. Kawi, *Appl. Catal. B* 50 (2004) 37.
- [21] B. Wichterlova, Z. Sobalik, J. Dedecek, *Appl. Catal. B* 41 (2003) 97.
- [22] Y. Traa, B. Burger, J. Weitkamp, *Microporous Mesoporous Mater.* 30 (1999) 3.
- [23] G. Bagnasco, M. Turco, C. Resini, T. Montanari, M. Bevilacqua, G. Busca, *J. Catal.* 225 (2004) 536.
- [24] J. Janas, T. Machej, J. Gurgul, L.P. Socha, M. Che, S. Dzwigaj, *Appl. Catal. B* 75 (2007) 239.
- [25] F. Kapteijn, G. Marban, I. Rodriguez-Mirasol, J.A. Moulijn, *J. Catal.* 167 (1997) 256.
- [26] E.M. El-Malki, R.A. van Santen, W.M.H. Sachtler, *J. Catal.* 196 (2000) 212.
- [27] A.H. Øygarden, J. Pérez-Ramírez, *Appl. Catal. B* 65 (2006) 163.
- [28] J. Pérez-Ramírez, A. Gallardo-Llamas, *Appl. Catal. A* 279 (2005) 117.
- [29] Y. Li, J.N. Armor, *Appl. Catal. B* 1 (1992) L31.
- [30] Y. Li, J.N. Armor, *J. Catal.* 150 (1994) 376.
- [31] X. Wang, H.Y. Chen, W.M.H. Sachtler, *J. Catal.* 19 (2001) 281.
- [32] L.J. Lobree, A.W. Aylor, J.A. Reimer, A.T. Bell, *J. Catal.* 169 (1997) 188.
- [33] T. Beutel, B.J. Adelman, W.M.H. Sachtler, *Appl. Catal. B* 9 (1996) L1.

- [34] K. Hadjiivanov, B. Tsyntsarski, T. Nikolova, *Phys. Chem. Chem. Phys.* 1 (1999) 4521.
- [35] M.C. Campa, S. de Rossi, G. Ferraris, V. Indovina, *Appl. Catal. B* 8 (1996) 315.
- [36] K. Hadjiivanov, M. Mihaylov, *J. Chem. Soc., Chem. Commun.* (2004) 2200.
- [37] H. Hamada, Y. Kintaichi, M. Sasaki, T. Ito, *Appl. Catal.* 70 (1991) L15.
- [38] L. Descorme, P. Gelin, M. Primet, C. Lecuyer, *Catal. Lett.* 41 (1996) 133.
- [39] C. Resini, T. Montanari, L. Nappi, G. Bagnasco, M. Turco, G. Busca, F. Bregani, M. Notaro, G. Rocchini, *J. Catal.* 214 (2003) 179.
- [40] R. Brosius, J.A. Martens, *Topics Catal.* 28 (2004) 119.
- [41] X. Carrier, P. Lukinskas, S. Kuba, L. Stievano, F.E. Wagner, M. Che, H. Knozinger, *Chem. Phys. Chem.* 5 (2004) 1191.
- [42] G. Grosse, Mos90—Version 2. 2, Technische Universität München, Garching, Germany, 1992.
- [43] S. Dzwigaj, M.J. Peltre, P. Massiani, A. Davidson, M. Che, T. Sen, S. Sivasanker, *J. Chem. Soc., Chem. Commun.* (1998) 87.
- [44] S. Dzwigaj, M. Che, *J. Phys. Chem. B* 110 (2006) 12490.
- [45] M.A. Camblor, A. Corma, J. Pérez-Pariente, *Zeolites* 13 (1993) 82.
- [46] J.S. Reddy, A. Sayari, *Stud. Surf. Sci. Catal.* 94 (1995) 309.
- [47] M.S. Kumar, M. Schwidder, W. Gruenert, A. Brueckner, *J. Catal.* 227 (2004) 384.
- [48] A.M. Ferretti, A.-L. Barra, L. Forni, C. Oliva, A. Schweiger, A. Ponti, *J. Phys. Chem. B* 108 (2004) 1999.
- [49] A. Brueckner, R. Lück, W. Wieker, B. Fahlke, H. Mehner, *Zeolites* 12 (1992) 380.
- [50] D. Goldfarb, M. Bernardo, K.G. Strohmaier, D.E.W. Vaughan, H. Thomann, *J. Am. Chem. Soc.* 116 (1994) 6344.
- [51] P. Wenquin, O. Shilun, K. Zhiyun, P. Shaoyi, *Stud. Surf. Sci. Catal.* 49 (1989) 218.
- [52] A.F. Ojo, J. Dwyer, R.V. Parish, *Stud. Surf. Sci. Catal.* 49 (1989) 227.
- [53] E.A. Zhilinskaya, G. Delahay, M. Mauvezin, B. Coq, A. Aboukais, *Langmuir* 19 (2003) 3596.
- [54] A.A. Aboukais, E.A. Zhilinskaya, I.N. Filimonov, N.S. Nesterenko, S.E. Timoshin, I.I. Ivanova, *Catal. Lett.* 111 (2006) 97.
- [55] B. Wichterlova, L. Kubelkova, P. Jiru, D. Kolihova, *Collect. Czech. Chem. Commun.* 45 (1980) 2143.
- [56] G.K. Wertheim, J.P. Remeika, *Phys. Lett.* 10 (1964) 14.
- [57] V.G. Bhide, S.K. Date, *Phys. Rev.* 172 (1968) 345.
- [58] C. Jia, P. Massiani, D. Barthomeuf, *J. Chem. Soc., Faraday Trans.* 89 (1993) 3659.
- [59] S. Dzwigaj, L. Stievano, F.E. Wagner, M. Che, *J. Phys. Chem. Solids* 68 (2007) 1885.
- [60] G. Centi, G. Gollinetti, G. Busca, *J. Phys. Chem.* 94 (1990) 6813.
- [61] G. Busca, G. Centi, F. Trifiro, Y. Lorenzelli, *J. Phys. Chem.* 90 (1986) 1337.
- [62] H. Knözinger, *Adv. Catal.* 25 (1976) 184.
- [63] A.D. Cowan, N.W. Cant, B.S. Haynes, P.F. Nelson, *J. Catal.* 176 (1988) 329.
- [64] N.W. Cant, I.O.Y. Liu, *Catal. Today* 63 (2000) 133.
- [65] R. Burch, J.P. Breen, F.C. Meunier, *Appl. Catal. B* 39 (2002) 283.
- [66] V.A. Sadykov, V.V. Lunin, V.A. Matyshak, E.A. Paukshtis, A.Ya. Rozovskii, N. Bulgakov, J.R.H. Ross, *Kinet. Catal.* 44 (2003) 379.